13. Vanoni, V. A., and G. N. Nomicos, *Trans. Am. Soc. Civil Engrs.*, **125**, 1140 (1960).
14. Lapple, C. E., "Chemical Engineering Handbook," p. 1019, 3 ed., J. H. Perry, ed., McGraw-Hill, New York (1950).
15. von Karman, Theodore, *J. Aeronaut. Sci.*, **1**, 1 (1934).
16. Bagnold, R. A., *Brit. J. Appl. Phys.*, **2**, 29 (1951).
17. Adam, Otto, *Chemie-Ing.-Tech.*, **29**, 151 (1957).
18. Torobin, L. B., and W. H. Gauvin, *Can. J. Chem. Eng.*, **38**, 142 (1960).
19. Soo, S. L., and C. L. Tien, *J. Appl. Mech.*, **27**, 5 (1960).
20. Irmay, S., *J. Basic Eng.*, **82**, 961 (1960).
21. Laufer, John, *Natl. Advisory Comm. Aeronaut. 1174* (1954); see J. O. Hinze, "Turbulence," pp. 520-533, McGraw-Hill, New York (1960).
22. Steinour, H. H., *Ind. Eng. Chem.*, **36**, 618-624, 840-847, 901-907 (1944).
23. Richards, R. H., *Trans. Am. Inst. Mining Engrs.*, **38**, 210 (1907).
24. Bagnold, R. A., "The Physics of Blown Sands and Desert Dunes," Methuen, London, England (1941).
25. Taylor, G. I., *Proc. Roy. Soc.*, **A223**, 446 (1954).
26. Kline, S. J., and P. W. Runstadler, *J. Appl. Mech.*, **26**, 166 (1959).
27. Clarke, R. H., et al., *Trans. Inst. Chem. Engrs.*, **30**, 209 (1952).
28. Mehta, N. C., et al., *Ind. Eng. Chem.*, **49**, 986-992 (1957).
29. Zenz, F. A., *ibid.*, **41**, 2801 (1949).
30. Yufin, A. P., *Izvest. Akad. Nauk Usbekh SSR, Ser Tekh. Nauk*, No. 8, 1146 (1949).
31. Howard, G. W., *Trans. Am. Soc. Civil Engrs.*, **64**, 1377 (1938).
32. Silin, N. A., *Akad. Nauk URSR Kiev Dopovidi.*, **3**, 175-177 (1958).
33. Rose, H. E., and H. E. Barnacle, *The Engineer*, 898-901, 939-941 (June 14 and June 21, 1957).
34. Pogosoyan, M. G., *Gidrotekh. Stroit*, **27**, 39-42 (1958).
35. White, C. M., *Proc. Royal Soc.*, **174A**, 322-338 (1940).

Manuscript received September 26, 1961; revision received December 6,1961; paper accepted December 6, 1961. Paper presented at A.I.Ch.E. Baltimore meeting.

Steady Flow of an Oldroyd Viscoelastic Fluid in Tubes, Slits, and Narrow Annuli

MICHAEL C. WILLIAMS and R. BYRON BIRD

University of Wisconsin, Madison, Wisconsin

RHEOLOGICAL MODELS

One of the objectives of rheology is the development of generalized models to describe the mechanical behavior of classes of real liquids in a wide variety of steady and unsteady state conditions. Attempts to do this have been little more than constructions of empirical models to fit experimental data. Generalized Newtonian functions such as the power-law, Bingham, and Reiner-Philippoff functions (*1, 5, 23*) are found to describe steady flow of some materials in several simple geometries. However their use is usually restricted to a rather narrow range of steady flow conditions. Furthermore it is doubtful whether model parameters determined in one kind of viscometer would agree with those found in another type of viscometer. For example Fredrickson (*5*) found that the power-law constants obtained from tube flow data were *not* in general valid for axial flow in a coaxial cylindrical annulus.

A basic weakness of these generalized Newtonian models is their failure to account for elastic phenomena. Such effects have been tentatively described by functions which involve time derivatives of varied significance, as listed in Table 1. The standard linear viscoelastic models utilize only $\partial/\partial t$ and are inappropriate in situations where significant inertial forces exist. Recently several rheological models have been proposed which use more general time derivatives (see Table 1), and which are intended to combine and extend previous viscoelastic and non-Newtonian models. Some of these are shown in Table 2.* In that table each model is given in the forms $0 = F\ (\tau_{ik},\ \epsilon_{ik})$; the terms present in the function F are indicated by denoting the constant and operator multipliers associated with them. For example the De Witt model is $\left(1 + \lambda_1 \frac{\mathcal{D}}{\mathcal{D}t}\right) \tau_{ik} + 2\eta_0\, \epsilon_{ik} = 0$. The quantities λ_1, λ_2, κ_1, κ_2, μ_0, μ_1, μ_2, ν_1, ν_2 are constants with dimensions of time, η is a variable viscosity (g. cm.$^{-1}$ sec.$^{-1}$), and η_0 is a zero-shear viscosity.

* See also reference *13* for an analytical comparison of several rheological models.

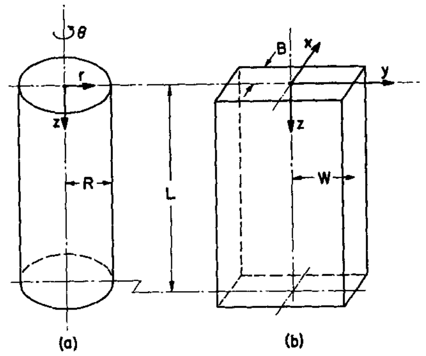

Fig. 1. (*a*) Cylindrical geometry; (*b*) plane slit geometry.

In Tables 1 and 2 Cartesian tensors are used with the usual summation convention. The quantities τ_{ik} are the components of the shear-stress tensor. The rate-of-strain tensor ϵ_{ik} and vorticity tensor ω_{ik} are defined in the usual way:

$$\epsilon_{ik} = \frac{1}{2}\left(\frac{\partial v_k}{\partial x_i} + \frac{\partial v_i}{\partial x_k}\right); \qquad \omega_{ik} = \frac{1}{2}\left(\frac{\partial v_k}{\partial x_i} - \frac{\partial v_i}{\partial x_k}\right) \quad (1)$$

Experimental testing of the newer viscoelastic models has been somewhat limited in scope. Model (*d*) has been reported to be successful in describing the response of certain dilute polymer solutions to small-amplitude oscillation (*17, 20, 30*). Model (*e*) predicts incorrectly the normal stresses present

TABLE 1. TIME DERIVATIVES OF A SECOND-ORDER CARTESIAN TENSOR, $\tau_{i\kappa}$

Symbol	Reference	Expanded form, referred to stationary axes	Significance
$\frac{\partial \tau_{i\kappa}}{\partial t}$		$\frac{\partial \tau_{i\kappa}}{\partial t}$	Time rate of change of $\tau_{i\kappa}$, observed from fixed coordinates referred to stationary axes.
$\frac{D\tau_{i\kappa}}{Dt}$	1, 18	$\frac{\partial \tau_{i\kappa}}{\partial t} + v_m \frac{\partial \tau_{i\kappa}}{\partial x_m}$	Time rate of change of $\tau_{i\kappa}$, observed from coordinates fixed with reference to axes being translated rigidly with the fluid.
$\frac{\mathcal{D}\tau_{i\kappa}}{\mathcal{D}t}$	4, 18, 23a	$\frac{D\tau_{i\kappa}}{Dt} + \omega_{im}\tau_{m\kappa} + \omega_{\kappa m}\tau_{im}$	Time rate of change of $\tau_{i\kappa}$, observed from coordinates fixed with reference to axes being translated and rotated rigidly with the fluid.
$\frac{\mathfrak{d}\tau_{i\kappa}}{\mathfrak{d}t}$	16, 18, 24	$\frac{\mathcal{D}\tau_{i\kappa}}{\mathcal{D}t} + \epsilon_{im}\tau_{m\kappa} + \epsilon_{\kappa m}\tau_{im}$	Time rate of change of $\tau_{i\kappa}$, observed from coordinates fixed with reference to axes being translated, rotated, and deformed with the fluid.

with steady flow in cone-and-plate (*12*) and rotating-parallel-plate equipment (*22*), and moreover yields a non-Newtonian viscosity expression which is unrealistic at very high shear rates. Models (*a*) and (*b*) were shown (*16, 17, 18*) to predict a properly behaved viscosity and such normal stress phenomena as the Weissenberg effect. Model (*a*) has been used to calculate the drag force for the creeping flow around a sphere; comparison of calculated results with a limited amount of experimental data suggests that the model is adequate at low flow rates (*11*). This model has also been used for a semiquantitative description of the normal stresses associated with the swelling of jets (*15*); only limited information about model (*a*) can be obtained from the tentative theory presented, inasmuch as the power law was used to give the velocity distribution. Model (*j*) has been applied to the description of steady helical flow, but no comparisons with experiment are available (*6, 26*).

STEADY FLOW IN A CIRCULAR TUBE

Consider an Oldroyd liquid, described by model (*a*). When one uses r, θ, z-coordinates (Figure 1*a*), it may be postulated that $p = p(r,z)$ and that the only nonzero component of the velocity is the axial one, $v_z = v_z(r)$. Hence $\epsilon_{rz} = \epsilon_{zr} = (1/2)(dv_z/dr)$ and $\omega_{rz} = -\omega_{zr} = (1/2)(dv_z/dr)$. All other ϵ_{ik} and ω_{ik} are zero.

Use of model (*a*), with these postulates for axial tube flow, leads to expressions for τ_{rr}, $\tau_{\theta\theta}$, τ_{zz}, and τ_{rz} which have been given elsewhere (*18*). Specifically it has been shown that τ_{rz} is

$$\tau_{rz} = \eta_0 \left(\frac{1 + a\gamma^2}{1 + b\gamma^2} \right) \gamma \qquad (2)$$

in which $\gamma = (-\, dv_z/dr)$ and

$$a = \left[\lambda_1\lambda_2 + \mu_0 \left(\mu_2 - \frac{3}{2}\nu_2 \right) - \mu_1 \left(\mu_2 - \nu_2 \right) \right] \qquad (3)$$

$$b = \left[\lambda_1^2 + \mu_0 \left(\mu_1 - \frac{3}{2}\nu_1 \right) - \mu_1 \left(\mu_1 - \nu_1 \right) \right] \qquad (4)$$

The function in Equation (2) has the following properties: it approaches Newtonian form with a zero-shear viscosity η_0 if γ is small, and is Newtonian if $a/b = 1$. At large γ it indicates a limiting viscosity $\eta_\infty = (a/b)\eta_0$. For moderate γ it indicates dilatancy if $a/b > 1$ and pseudoplasticity if $a/b < 1$.

FLOW RATE IN A CIRCULAR TUBE

Integration of the z-component of the equation of motion (*1*)

$$0 = -\frac{\partial p}{\partial z} - \frac{1}{r}\frac{d}{dr}(r\tau_{rz}) + \rho g_z \qquad (5)$$

leads to the stress distribution

$$\tau_{rz} = \frac{1}{2} Pr \qquad (6)$$

where $P \equiv (\Delta p/L) + \rho g_z$. Combination with Equation (2) yields

$$r = \frac{2\eta_0}{P} \left(\frac{1 + a\gamma^2}{1 + b\gamma^2} \right) \gamma \qquad (7)$$

TABLE 2. RHEOLOGICAL MODELS: $F(\tau_{i\kappa}, \epsilon_{i\kappa}) = 0$

	Model	$\tau_{i\kappa}$	$\epsilon_{i\kappa}$	$-(\epsilon_{im}\tau_{m\kappa} + \epsilon_{m\kappa}\tau_{im})$	$-\epsilon_{im}\epsilon_{m\kappa}$	$\epsilon_{i\kappa}\tau_{mm}$	$\epsilon_{mn}\tau_{mn}\delta_{i\kappa}$	$\epsilon_{mn}\epsilon_{mn}\delta_{i\kappa}$
(a)	Oldroyd (*18*)	$\left(1 + \lambda_1 \frac{\mathcal{D}}{\mathcal{D}t}\right)$	$2\eta_0\left(1 + \lambda_2 \frac{\mathcal{D}}{\mathcal{D}t}\right)$	μ_1	$4\eta_0\mu_2$	μ_0	ν_1	$2\eta_0\nu_2$
(b)	Oldroyd (*17*)*	$\left(1 + \lambda_1 \frac{\mathfrak{d}}{\mathfrak{d}t}\right)$	$2\eta_0\left(1 + \lambda_2 \frac{\mathfrak{d}}{\mathfrak{d}t}\right)$	$2\kappa_1$	$8\eta_0\kappa_2$			
(c)	Oldroyd (*16*)	$\left(1 + \lambda_1 \frac{\mathfrak{d}}{\mathfrak{d}t}\right)$	$2\eta_0\left(1 + \lambda_2 \frac{\mathfrak{d}}{\mathfrak{d}t}\right)$					
(d)	Jeffreys, (*8*) Fröhlich and Sack (*7*)	$\left(1 + \lambda_1 \frac{\partial}{\partial t}\right)$	$2\eta_0\left(1 + \lambda_2 \frac{\partial}{\partial t}\right)$					
(e)	DeWitt (*4*) Fromm (*8a*)	$\left(1 + \lambda_1 \frac{\mathcal{D}}{\mathcal{D}t}\right)$	$2\eta_0$					
(f)	Broer, (*2*) Kuvshinski (*10*)	$\left(1 + \lambda_1 \frac{D}{Dt}\right)$	$2\eta_0$					
(g)	Maxwell (*14*)	$\left(1 + \lambda_1 \frac{\partial}{\partial t}\right)$	$2\eta_0$					
(h)	Generalized Newton (*1*)‡	1	2η					
(i)	Newton (*1*)	1	$2\eta_0$					

(j) Rivlin-Erickson (*24, 25, 26*)

$$F = \tau_{i\kappa} + 2\alpha_1\epsilon_{i\kappa} + 2\alpha_2\dot{\epsilon}_{i\kappa} + 4\alpha_3\epsilon_{im}\epsilon_{m\kappa} + 4\alpha_4\dot{\epsilon}_{im}\dot{\epsilon}_{mk} + 4\alpha_5(\epsilon_{im}\dot{\epsilon}_{mk} + \dot{\epsilon}_{im}\epsilon_{m\kappa}) + 8\alpha_6(\epsilon_{im}\epsilon_{mn}\dot{\epsilon}_{n\kappa} + \dot{\epsilon}_{im}\epsilon_{mn}\epsilon_{n\kappa}) + 8\alpha_7(\epsilon_{im}\dot{\epsilon}_{mn}\dot{\epsilon}_{n\kappa} + \dot{\epsilon}_{im}\dot{\epsilon}_{mn}\epsilon_{n\kappa}) + 16\alpha_8(\epsilon_{im}\epsilon_{mn}\dot{\epsilon}_{np}\dot{\epsilon}_{p\kappa} + \dot{\epsilon}_{im}\dot{\epsilon}_{mn}\epsilon_{np}\epsilon_{p\kappa})$$

Note: $\dot{\epsilon}_{i\kappa} \equiv \mathfrak{d}\epsilon_{i\kappa}/\mathfrak{d}t$, and higher convected derivatives of $\epsilon_{i\kappa}$ are assumed to be zero; the α_i are functions of the ten scalar invariants involving $\epsilon_{i\kappa}$ and $\dot{\epsilon}_{i\kappa}$.

* To compare with model (a): $2\kappa_1 = \lambda_1 + \mu_1$ and $2\kappa_2 = \lambda_2 + \mu_2$.
‡ η is a function of the scalar invariants of ϵ_{ik}.

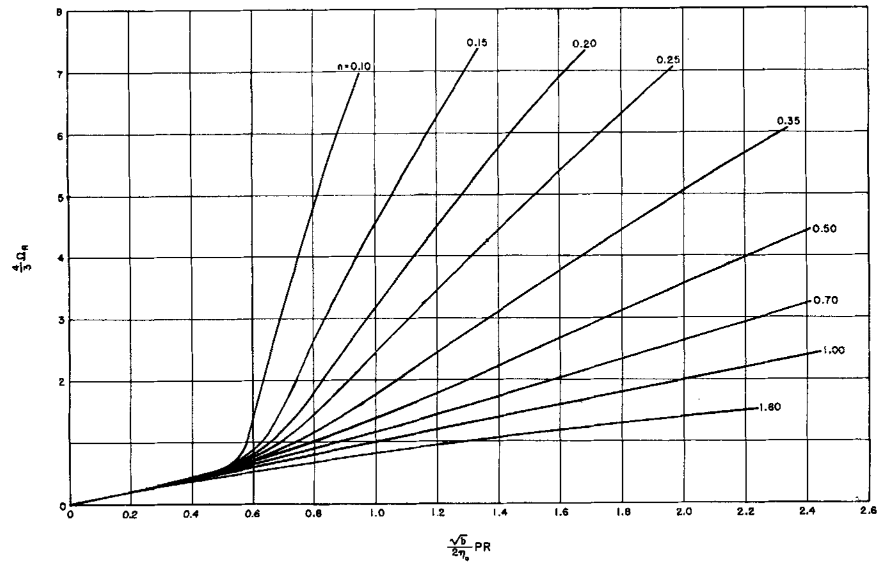

Fig. 2. Volumetric flow rate vs. pressure drop for an Oldroyd liquid in a cylindrical tube, calculated from Equations (10), (11), and (12). Here (4/3) $\Omega_R = \sqrt{b}\,(4Q/\pi R^3)$, with flow rate Q and tube radius R. Also $P = (\Delta p/L) + \rho g_z$ is the effective pressure gradient, η_0 is the zero-shear viscosity, and $n = a/b$ is a ratio of combinations of time constants.

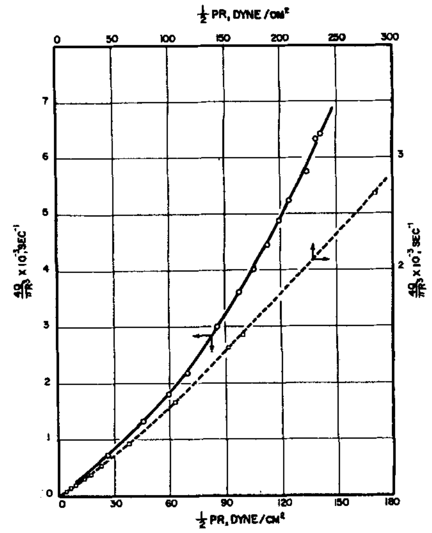

Fig. 4. Plot of $4Q/\pi R^3$ vs. $PR/2$. Squares represent Slattery's data (27) for 4.0% aqueous carboxymethylcellulose (low) at 85°F. The dashed line is a curve fit from Figure 2 with $n = a/b = 0.67$, $b = 2.53 \times 10^{-4}$ sec², and $\eta_0 = 1.52$ poise. Circles represent data of Chu, Burridge, and Brown[3] for 0.025% aqueous sodium polymethacrylate at 50°C. The solid line is a curve fit from Figure 2 with $n = a/b = 0.50$, $b = 1.04 \times 10^{-7}$ sec², and $\eta_0 = 0.029$ poise. These comparisons illustrate the utility of the Oldroyd models at low flow rates.

The volumetric flow rate is given by

$$Q = 2\pi \int_0^R v_z(r)\, r\, dr = \frac{\pi}{3}\left(R^3\gamma_R - \int_0^{\gamma_R} r^3\, d\gamma\right) \quad (8)$$

where R is the tube radius and γ_R is $(-\,dv_z/dr)$ evaluated at $r = R$. This form for Q is obtained by two successive integrations by parts, as reported in (*26*) and on page 70 (*1*). Substitution of $r(\gamma)$ from Equation (7) into Equation (8) then gives

$$Q = \frac{\pi R^3 \gamma_R}{3} - \frac{\pi}{3}\left(\frac{2\eta_0}{P}\right)^3 \cdot \int_0^{\gamma_R}\left(\frac{1 + a\gamma^2}{1 + b\gamma^2}\right)^3 \gamma^3\, d\gamma \quad (9)$$

It is convenient to express the result of the integration in terms of the dimensionless quantities $\Omega_R = 3\sqrt{b}\; Q/\pi R^3$, $X_R = b\gamma_R^2$, and $n = a/b$:

$$\Omega_R = \left[\, 1 - \frac{1}{2X_R^2}\left(\frac{1 + X_R}{1 + nX_R}\right)^3 f_R \,\right]\sqrt{X_R} \quad (10)$$

in which

$$f_R = \frac{1}{2} n^3 X_R^2 - 3n^3(n-1)X_R + 3n(n-1)(2n-1)\ln(1 + X_R) - \frac{1}{2} X_R\left(\frac{n-1}{1 + X_R}\right)^2 [6n + (7n-1)X_R] \quad (11)$$

To obtain Ω_R as a function of P it is necessary to eliminate X_R from the above result by using the following relation, which is Equation (7) evaluated at $r = R$:

$$\frac{\sqrt{b}}{2\eta_0} PR = \left(\frac{1 + nX_R}{1 + X_R}\right)\sqrt{X_R} \quad (12)$$

In this way Figure 2 has been prepared with an IBM-1620. The plot given there corresponds to the traditional flow curves in which $4Q/\pi R^3$ is given as a function of $PR/2$. Note that for $n < 1$ a curve similar to that for an Ostwald liquid (*19, 21*) is exhibited, and for small $n(= 0.1)$ a Bingham plastic flow curve is approximated. It is seen explicitly from Equations (10), (11), and (12) how the viscoelastic properties of the fluid affect the steady flow behavior in a tube.

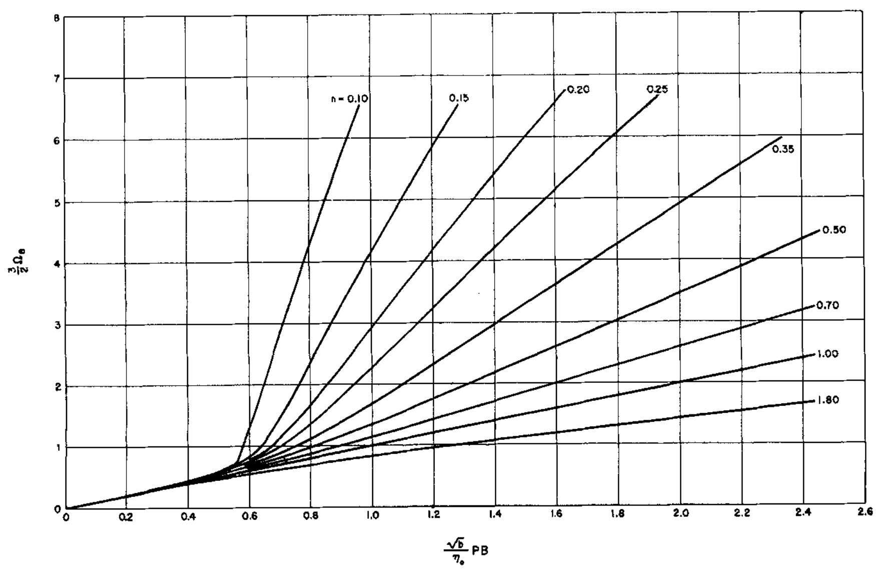

Fig. 3. Volumetric flow rate vs. pressure drop for an Oldroyd liquid in a plane slit, calculated from Equations (13, (14), and (15). Here (3/2) $\Omega_B = \sqrt{b}\,(3\;Q/4WB^2)$, with flow rate Q, slit width $2W$, and slit thickness $2B$ ($W >> B$). Also $P = (\Delta p/L) + \rho g_z$ is the effective pressure gradient, η_0 is the zero-shear viscosity, and $n = a/b$ is a ratio of combinations of time constants.

STEADY FLOW IN A PLANE SLIT AND A NARROW ANNULUS

By steps completely analogous to the above development one obtains an expression for flow rate in a thin plane slit of thickness $2B$ and width $2W$ (Figure 1*b*). The results may be conveniently expressed in terms of dimensionless quantities $\Omega_B \equiv \sqrt{b}\; Q/2WB^2$, $X_B \equiv b(-dv_z/dx)^2_{x=B}$, and $n = a/b$:

$$\Omega_B = \left[\, 1 - \frac{1}{2X_B}\left(\frac{1 + X_B}{1 + nX_B}\right)^2 f_B \right]\sqrt{X_B} \quad (13)$$

in which

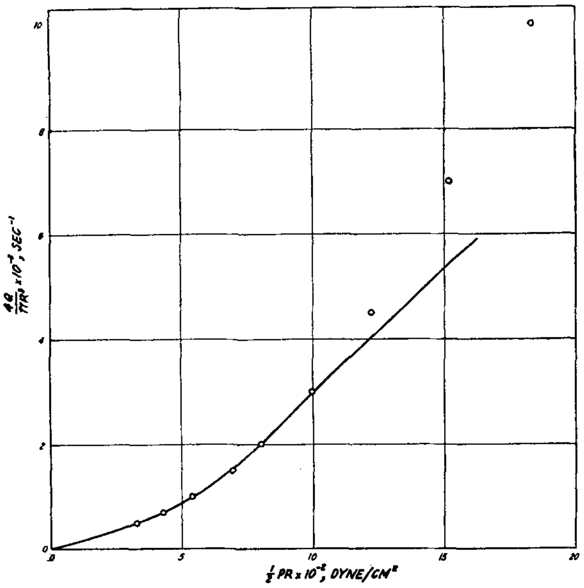

Fig. 5. Plot of $4Q/\pi R^3$ vs. $PR/2$. Circles represent Fredrickson's data (5) for 2.5% aqueous carboxymethylcellulose (medium) at 85°F. The solid line, a curve fit from Figure 2 with $n = a/b = 0.35$, $b = 7.70 \times 10^{-5}$ sec.², and $\eta_0 = 7.01$ poise, illustrates the shortcomings of the Oldroyd models over large flow ranges.

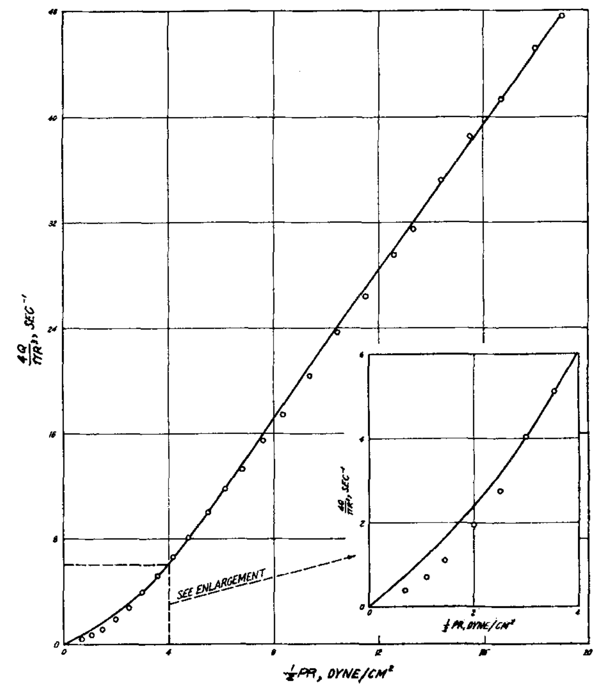

Fig. 6. Plot of $4Q/\pi R^3$ vs. $PR/2$. Circles represent data of Ostwald and Malss (19) for cholesterylbutyrate at 100°C. The solid line, taken from Figure 2 with $n = a/b = 0.45$, $b = 0.0297$ sec.², and $\eta_0 = 0.862$ poise, is an attempt to fit an entire flow curve. Note particularly the failure near zero shear (inset).

$$f_B = \frac{2}{3} n^2 X_B + (5n-1)(n-1) \cdot \frac{\tan^{-1}\sqrt{X_B}}{\sqrt{X_B}} - (n-1) \cdot \left[4n + \left(\frac{n-1}{1+X_B} \right) \right] \quad (14)$$

Furthermore, to complete the results, one needs the relation between P and X_B

$$\frac{\sqrt{b}}{\eta_0} PB = \left(\frac{1+nX_B}{1+X_B} \right) \sqrt{X_B} \quad (15)$$

to get Q as a function of P. The resulting curves, computed on an IBM-1620, are shown in Figure 3.

The results in Figure 3 may be used for the approximate description of the axial flow of an Oldroyd fluid in the thin annular space between two cylinders of radii R_i and R_o ($R_i < R_o$ and $R_i \approx R_o$). One needs only to replace $2B$ by $(R_o - R_i)$ and W by $\pi(R_o + R_i)$.

VELOCITY PROFILES

Expressions for Q vs. P for tubes and slits were obtained without first deriving the velocity profiles explicitly. For some analyses (for example swelling of jets) it might be useful to have $v_z(r)$ for tube flow and $v_z(x)$ for slit flow.

For tube flow the velocity may be found from Equation (7)

$$v_z = \int_r^R \gamma\, dr = \frac{2\eta_0}{P} \int_\gamma^{\gamma_R} \gamma \left[\frac{1 + (3a-b)\gamma^2 + ab\gamma^4}{(1+b\gamma^2)^2} \right] d\gamma \quad (16)$$

where $\gamma = (-dv_z/dr)$ as before. Integration then gives the dimensionless velocity $(\sqrt{b}/R)v_z$ as a function of dimensionless distance r/R by elimination of X between the following two equations:

$$\frac{\sqrt{b}}{R} v_z = \frac{1}{2X_R} \left(\frac{1+X_R}{1+nX_R} \right) \cdot \left[n\,(X_R - X) + (n+1) \ln\left(\frac{1+X_R}{1+X} \right) - 2\,(n-1) \left(\frac{1}{1+X} - \frac{1}{1+X_R} \right) \right] \quad (17)$$

$$\frac{r}{R} = \left(\frac{1+nX}{1+X} \right) \left(\frac{1+X_R}{1+nX_R} \right) \cdot \sqrt{\frac{X}{X_R}} \quad (18)$$

The second of these equations is just the quotient of Equations (7) and (12). To get $v_z(x)$ for slit flow Equations (17) and (18) can be used by replacing R by B and r by x.

COMPARISON WITH EXPERIMENT

The predictions of Equations (10), (11), and (12) were tested with tube flow data involving the following liquids: 4.0% aqueous carboxymethylcellulose (low) (*29*), Figure 4; 0.025% aqueous sodium polymethacrylate (3), Figure 4; 2.5% aqueous carboxymethylcellulose (medium), Figure 5; and cholesterylbutyrate (*21*), Figure 6. Inasmuch as Oldroyd proposed his models for use at relatively low stresses and shear rates, it is not surprising that Figure 4 shows good fits. Indeed with three adjustable constants, η_0, a, b, the Oldroyd equations should be capable of reproducing the initial regions of nearly all flow curves. The curve fits were obtained by first selecting from Figure 2 a curve with parameter n whose shape appeared most closely to resemble that of the data, and then adjusting the scale factors $\sqrt{b}$ and $\sqrt{b}/\eta_0$ to superimpose the two. Thereafter the process was repeated for different n values until the most satisfying choice was obtained. The validity of this approach is indicated by the agreement of the value of η_0 so obtained, with that derived from extrapolation of η to zero shear. For example from the dashed curve of Figure 4 one gets $\eta_0 = 1.52$ poise, whereas extrapolation (*31*) yields $\eta_0 = 1.59 \pm 0.02$.

When a larger range of data is considered, as in Figure 5, the limitations of the model become apparent. Although the fit is satisfactory at low stresses, it is obviously inadequate for $PR/2 > 1{,}000$ dyne/sq. cm. It was found for a number of liquids that even if data at low stresses were well represented by a curve from Figure 2, the latter would fail at high stresses in the manner shown by Figure 5.

An attempt to duplicate an entire Ostwald curve is presented in Figure 6. The solid line is but one of several which might be drawn. It appears to have no more significance than any empirical fit, as suggested by the poor agreement at lower stresses (see inset). Thus in this instance η_0 cannot be interpreted in the usual way as a zero-shear viscosity. Observation of several Ostwald flow curves (*21*) for a variety of materials revealed that their shapes were subtly but fundamentally different from the curves of Figure 2.

CONCLUSION

Since the Oldroyd models were developed under the assumption that terms higher than second order (for example terms containing $\partial^2/\partial t^2$) were negligible, a fair test of them is with flow data taken at relatively low stresses. Therefore the results given here are thought to be in encouraging agreement with experiment.

The constants a and b obtained from capillary flow curves involve all the time constants of the original model. Additional information is needed to evaluate the time constants separately. Normal pressure measurements of Roberts (*27*) in a cone-and-plate geometry indicate that normal stresses in the plane perpendicular to the flow direction are equal. (For example $\tau_{rr} = \tau_{\theta\theta}$ in axial tube flow.) The equality of these normal stresses imposes a further restriction on the constants in the Oldroyd models: for model (a), $\mu_1 = \lambda_1$ and $\mu_2 = \lambda_2$; for model (b), $\lambda_1 = \kappa_1$ and $\lambda_2 = \kappa_2$. These qualities cause model (b) to lose its ability to predict non-Newtonian viscosity. On the other hand model (a) remains satisfactory in this respect, and a and b contain only λ_1, λ_2, ν_1, ν_2, and μ_0. Of these, λ_1 and λ_2 can be found through small-amplitude oscillatory experiments (*20, 30*) or (in principle) through cone-and-plate normal pressure measurements (*12*). If the remaining three unknown constants could be evaluated, model (a) would be experimentally determined.

Oldroyd's model is intended only to be a simple tensor generalization of the Jeffreys model (d). Nonetheless its predictions of normal stresses, non-Newtonian viscosity, and time-dependent viscoelastic behavior are in qualitative accord with physical observations. Its extension to include higher-order time derivatives and cross terms would lead to more flexible viscosity expressions capable of describing real materials over large ranges of data. Of course this implies the introduction of still more constants.

ACKNOWLEDGMENT

The authors wish to express their appreciation for the financial support of National Science Foundation Grant G-11996; in addition we wish to thank Messrs. T. J. Sadowski, J. L. Sutterby, and A. J. Ziegenhagen of our department for helpful suggestions and aid in making available some of the data presented here. Professor R. S. Schechter (University of Texas) and Dr. J. C. Biery (University of Wisconsin) read the manuscript very thoroughly and contributed several valuable ideas. An advance copy of a manuscript (*7*) by Professor A. G. Fredrickson (Chemical Engineering Department, University of Minnesota) stimulated our interest in the Oldroyd models. Figures 2 and 3 were prepared with the help of the facilities of the Wisconsin Engineering Digital Computer Laboratory.

NOTATION

a,b = groupings of parameters of the Oldroyd models
B = half-thickness of a plane slit, see Figure 1*b*
f_R,f_B = functions of shear rates, see Equations (11) and (14)
g_z = gravitational acceleration in z-direction
L = length of tube and slit, see Figure 1
n = a/b
P = $\Delta p/L + \rho g_z$
Q = volumetric flow rate
r = radial tube coordinate, see Figure 1*a*
R = tube radius, see Figure 1*a*
t = time
$v_z(r)$ = component of the axial velocity vector
$v_z(x)$ = component of the longitudinal velocity vector
W = half-width of a plane slit, see Figure 1*b*
x = lateral coordinate of a plane slit, see Figure 1*b*
X_R,X_B = dimensionless shear rates at the wall
z = axial tube coordinate; longitudinal slit coordinate, see Figure 1

Greek Letters

α_j = functions of shear-rate invariants, in model (j)
γ = shear rate, $-dv_z/dr$ or $-dv_z/dx$
γ_B = shear rate at the slit wall
γ_R = shear rate at the tube wall
δ_{ik} = Kronecker delta
ϵ_{ik} = component of shear-rate tensor, see Equation (1)
κ_1,κ_2 = constants in model (b)
λ_1,λ_2 = constants in model (b), and others
η = non-Newtonian viscosity
η_0 = limiting viscosity at low shear
η_∞ = limiting viscosity at high shear
ν_1,ν_2 = constants in model (a)
μ_0,μ_1,μ_2 = constants in model (a)
ρ = liquid mass density
τ_{ik} = component of shear-stress tensor (called $-p'_{ik}$ by Oldroyd)
ω_{ik} = component of vorticity tensor, see Equation (1)
Ω_R = dimensionless flow rate in a circular tube, $3\sqrt{b}\, Q/\pi R^3$
Ω_B = dimensionless flow rate in a plane slit, $\sqrt{b}\, Q/2WB^2$

LITERATURE CITED

1. Bird, R. B., W. E. Stewart, and E. N. Lightfoot, "Transport Phenomena," Wiley, New York (1960).
2. Broer, L. J. F., *Appl. Sci. Research*, **A6**, 226 (1956-57).
3. Chu, Ju Chin, K. C. Burridge, and Frank Brown, *Chem. Eng. Sci.*, **3**, 229 (1954).
4. DeWitt, T. W., *J. Appl. Phys.*, **26**, 889 (1955).
5. Fredrickson, A. G., Ph.D. thesis, Univ. Wisconsin, Madison, Wisconsin (1959).
6. ———, *Chem. Eng. Sci.*, **11**, 252 (1960).
7. ———, unpublished manuscript.
8. Frölich, H., and R. Sack, *Proc. Roy. Soc. (London)*, **A185**, 415 (1946).
8a. Fromm, H., *ZAMM*, **25**, 146 (1947).
9. Jeffreys, H., "The Earth," 2 ed., p. 265, Cambridge Univ. Press, Cambridge, England (1929).
10. Kuvshinski, E. V., *J. Exptl. Theoret. Phys. (U.S.S.R.)*, **21**, 88 (1951).
11. Leslie, F. M., and R. I. Tanner, *Quart. J. Mech. Appl. Math.*, **14**, 36 (1961).
12. Markovitz, Hershel, and R. B. Williamson, *Trans. Soc. Rheol.*, **1**, 15 (1957).
13. Markovitz, Hershel, *ibid.*, p. 25.
14. Maxwell, J. C., *Trans. Roy. Soc. (London)*, **157**, 49 (1867).
15. Metzner, A. B., E. L. Carley, and I. K. Park, *Modern Plastics*, **37**, 133 (1960).
16. Oldroyd, J. G., *Proc. Roy. Soc. (London)*, **A200**, 523 (1950).
17. ———, *Quart. J. Mech. Appl. Math.*, **4**, 271 (1951).
18. ———, *Proc. Roy. Soc. (London)*, **A245**, 291 (1958).
19. ———, "Rheology," Vol. 2, Chap. 16, F. R. Eirich, ed., Academic Press, New York (1956).
20. ———, D. J. Strawbridge, and B. A. Toms, *Proc. Phys. Soc.*, **B64**, 44 (1951).
21. Ostwald, W., and H. Malss, *Kolloid-Z.*, **63**, 61, 192, 305 (1932-33).
22. Padden, F. J., and T. W. DeWitt, *J. Appl. Phys.*, **25**, 1086 (1954).
23. Philippoff, Wladimir, "Viscosität der Kolloide," Steinkopff, Dresden, Germany (1942).
23a. Prager, W., "Introduction to Mechanics of Continua," p. 155, Ginn, Chicago, Illinois (1961).
24. Rivlin, R. S., and J. L. Erickson, *J. Rat. Mech. Anal.*, **4**, 329 (1955).
25. Rivlin, R. S., *ibid.*, p. 681.
26. *Ibid.*, **5**, 179 (1956).
27. Roberts, J. E., "Proceedings Second International Congress Rheology," p. 91, Oxford Univ. Press, Cambridge, England (1953).
28. Sisko, A. W., *Ind. Eng. Chem.*, **50**, 1789 (1958).
29. Slattery, J. C., Ph.D. thesis, Univ. Wisconsin, Madison, Wisconsin (1959).
30. Toms, B. A., and D. J. Strawbridge, *Trans. Faraday Soc.*, **49**, 1225 (1953).
31. Ziegenhagen, A. J., unpublished work, Univ. Wisconsin, Madison, Wisconsin (1960).

Manuscript received July 11, 1961; revision received November 2, 1961; paper accepted November 6, 1961.